AD-A129 045 HYBRID EXPERIMENTAL-NUMERICAL STRESS ANALYSIS(U) 1/1
WASHINGTON UNIV SEATTLE DEPT OF MECHANICAL ENGINEERING
A S KOBAYASHI APR 83 UWA/DME/TR-83/47 N00014-76-C-0060
UNCLASSIFIED F/G 14/2 NL

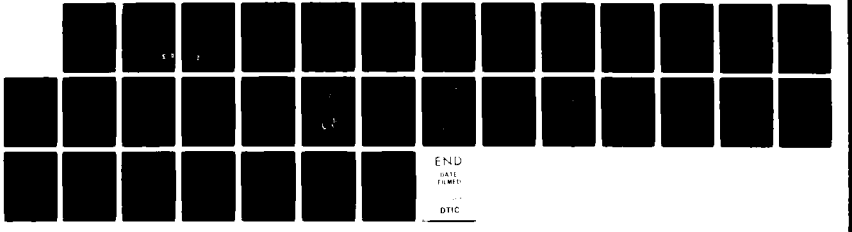

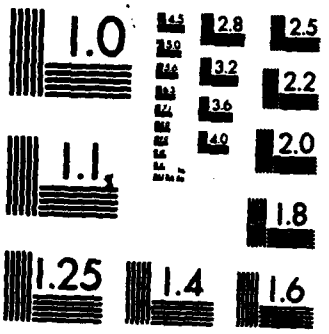

(12)

Office of Naval Research

Contract N00014-76-0060 NR 064-478

Technical Report No. UWA/DME/TR-83/47

HYBRID EXPERIMENTAL-NUMERICAL STRESS ANALYSIS

by

A. S. Kobayashi

April 1983

The research reported in this technical report was made possible through support extended to the Department of Mechanical Engineering, University of Washington, by the Office of Naval Research under Contract N00014-76-C-0060 NR 064-478. Reproduction in whole or in part is permitted for any purpose of the United States Government.

Department of Mechanical Engineering

College of Engineering

University of Washington

HYBRID EXPERIMENTAL-NUMERICAL STRESS ANALYSIS

by

Albert S. Kobayashi
Department of Mechanical Engineering
Seattle, Washington 98195

ABSTRACT

The hybrid experimental-numerical stress analysis technique, which saw limited applications during the 1950's, has been resurrected with the vastly improved numerical techniques of the 1970's. By inputing the experimental results as initial and boundary conditions, modern computer codes can be executed in its generation and application modes to yield results which are unobtainable when only one of the two techniques is used. The hybrid technique thus exemplifies the complementary role of the experimental and numerical techniques.

INTRODUCTION

One of the frustrations of an experimental stress analyst is the lack of a universal experimental procedure which solves all problems. Referred to as his second principle, Durelli states that "Seldom does one method give a complete solution, with the most efficiency [1]". Examples of this second principle is seen in photoelastic coating and brittle coating techniques which require additional strain gage testing in locations of high stress concentration identified by these two techniques. The hybrid experimental-numerical stress analysis technique is an aberration of the above where numerical stress analysis replaces the second experimental method.

Early applications of the hybrid experimental-numerical stress analysis technique were limited to separations of two- and three-dimensional state of

stress in photoelastic specimens. The first stress invariant obtained through a finite difference solution to the compatability equation and the maximum shear stress distribution provided by the isochromatics yielded the two planar components of the principal stresses [2,3,4]. The shear-difference method [2,5] and the Filon's method [6,7] used the isochromatic and isoclinic data to integrate the equilibrium equations along a straight line and a stress trajectory, respectively. These single-purpose numerical techniques thus provided only the stresses along a specified integration path.

In contrast to the above, the modern super codes based on finite element method, boundary element method and finite difference method yield the complete states of stress, strain and displacement for the given constitutive relations and boundary and initial conditions. The uncertainty or the lack of knowledge in these given conditions, however, limited the accuracy of the otherwise voluminuous outputs of these super codes. Inaccurate numerical modeling procedures generated results with obvious errors and are credited for the resurgence of three dimensional photoelasticity in the 1970's. The hybrid experimental-numerical stress analysis technique of today reduces, if not eliminates, the above uncertainties in prescribed input conditions by using experimentally determined boundary and initial conditions. The output from the otherwise proven numerical techniques are either the constitutive relation or the complete states of displacement, strain and stress which cannot be readily extracted through the use of a single experimental technique in stress analysis. Thus, the hybrid experimental-numerical technique is an extremely efficient stress analysis technique which often provides more information than needed. The full potential of the hybrid technique, however, is yet to be exploited because of the historic dichotomy between the theoreticians-turned numerical analysts and the experimentalists.

In the following, the utility of the hybrid experimental-numerical stress analysis technique will be demonstrated by some stress analysis problems involving two- and three-dimensional structural components, biomechanics and fracture mechanics.

ELASTIC ANALYSIS OF STRUCTURAL COMPONENTS

The numerical techniques used in modern hybrid technique for structural analysis are vastly superior to their predecessors since they provide the entire states of stress, strain and displacements. As a straight forward extension of the classical hybrid technique, Rao [8] used measured temperature and surface traction data to solve, by the finite difference method, the Beltrami-Michell stress equations of compatiblity interior to an axisymmetric solid. Figure 1a shows the end retaining ring, which is shrink-fitted to the two ends of the vector and which is used to contain the end loops of rotor windings, in a turbo-generator. The distributions of hoop stress, which is generated by shrink fitting and the centrifugal force, obtained by the hybrid technique, three dimensional frozen stress photoelasticity and a two-dimensional analog are shown in Figure 1b. The utility of this hybrid technique is demonstrated by the author's quote of "The time-needed for the analysis is smaller than that required by the time-consuming and tedious shear-difference methods" [8].

Figure 2 shows a water turbine wheel and its curvilinear finite difference grid representation which was analyzed by Barishpolsky [9]. Frozen stress photoelasticity was used to determine the stress tensor on the complex boundaries. These boundary values were input to the curvilinear finite difference equations for three-dimensional elasticity where the number of equations equalled the number of nodes and thus reduced the computational time by

three to six folds over standard finite difference codes. The procedure is extended to steady state, three-dimensional problems where measured surface temperature must be input in addition to the measured surface tractions [10].

While the specialized codes used in the above hybrid techniques are computationally more efficient by design, off-shelf codes in finite element and boundary element methods are often used for sheer expediencies. For an elasto-static problem, the boundary element method is more computationally efficient and natural where the input data consists of experimentally determined boundary displacements and tractions. When used together with the double exposure, laser speckle interferometry, "the measured surface displacements become the input data needed in the boundary element method to calculate the traction vectors at specified points on the boundary [11]" as well as in the interior of the body. Moslehy and Ranson [11] demonstrated the utility of this hybrid technique by the excellant agreements in theoretically and experimentally obtained stresses interior to a cantilever beam with a transverse end load. In a similar application of the hybrid technique, Balas, Sladek and Drzik [12] used the double-aperture, laser speckle interferometry and demonstrated the advantage of the hybrid technique by analyzing only the region of interest of a plate-stiffened frame. In this case, the recorded displacements were input to a simplified boundary, which is represented by the dashed lines, of the frame structure shown in Figure 3. Boundary element method was used to determine the stress distributions along the three cross sections shown in Figure 4.

As a variation in the above mentioned hybrid technique, Umeagukwu, Peters and Ranson [13] used two-dimensional photoelasticity together with a boundary element code to optimize the filets in a doubled notch tension plate. The interior principal stresses obtained by the hybrid technique were used to

more evenly distribute the load along the net section and thus resulted in a better understanding of the fillet optimization problem.

CORNEO-SCLERAL ENVELOPE

The interocular pressure of a human eye is maintained at a nearly constant level of 15 - 20 mmHg through a complex physiological system involving the mechanical, biochemical and neurological responses of the eye [14]. When the outflow of the ocular fluid is restricted by pathological conditions, the ensuing increase in interocular pressure eventually results in glaucoma which is the direct cause of 13.5 % of the blindness in United States [15]. Tonometry monitors this interocular pressure by measuring the exterior mechanical response of the cornea which is indented or flattened by a tonometer plunger. The tonometer reading is thus affected by the mechanical response of the pressurized corneo-scleral envelope which is essentially a pressure vessel containing the optical and neurological components.

The mechanical properties of the cornea and sclera are difficult to obtain because of the small size, delicacy and natural curvature. The commonly used ocular rigidity [16], which relates the pressure and volume of the corneo-scleral envelope, is a global coefficient and is not suitable for analyzing the local deformation process under tonometer loading. Simple tension testings of excised strips of the cornea [17] and the sclera [18] yielded erroneous modulus of elasticity and Poisson's ratio by the loosening of the collagen fibrils from the soft mucopolysaccharide at the excised edges. In order to overcome the deficiencies of the above global and local approaches, Woo et al [19,20] developed a hybrid experimental-numerical procedure for determining the local mechanical property of an intact corneo-scleral envelope.

Woo's experimental procedure consisted of measuring the cornea and sclera deformations as well as the volume changes of pressurized anterior segments of enucleated human eyes. A flying spot scanner was used to measure the relative motions of two white targets on the cornea or sclera which were mounted on a McEwen-type chamber [21]. Woo's numerical procedure consisted of matching, through trial and error, the measured and computed deformations and volume changes. A pressurized axisymmetric finite element model of the anterior segment of the corneo-scleral envelope was used to execute the finite element code in its application mode for this purpose. The resultant isotropic, trilinear, elastic stress-strain relations obtained for this analog model of the corneo-scleral envelope is shown in Figure 5. These trilinear stress strain relations were incorporated into a finite element of the total eye which was used to calculate the nonlinear intraocular pressure-volume relation. The lack of bending rigidity in the cornea under the tonometer probe was modeled by artificially reducing the bending stiffness of the finite elements in the compression region. With this modification, excellent correlations between the calculated and published experimental results were obtained [20].

The membrane shell elements, which were later used to construct the corneo-scleral envelope, shown in Figure 6 [22], removed the above mentioned artificial reduction in bending rigidity in the solid elements used by Woo. Woo's experimental data [19] was re-evaluated by this membrane shell model which yielded slightly different distribution of elastic moduli along the corneo-scleral shell. Such differences demonstrates the inevitable interdependence of the experimental data and numerical modeling of the hybrid experimental-numerical technique where the finite element model is used as an analog model of the experiment [23].

The anterior portion of the membrane finite element model was then used to model the deformation process under tonometer loading. Figure 7 shows the computed and measured [24] relations of probe force versus probe area under applanation tonometry.

ELASTIC-PLASTIC FRACTURE MECHANICS

Fracture parameters governing elastic, elastic-plastic and dynamic fracture, with the exception of geometric quantities such as crack opening displacements and crack tip opening angles, cannot be measured directly. In practice, even the above geometric parameters are difficult to quantify and are often computed by using analog models of the crack. Strain energy release rate and stress intensity factor in linear elastic fracture mechanics, which is a well established analog model of the crack, can be computed accurately by using modern numerical codes. The various fracture packages for these codes have been verified by a recent benchmark problem [25] and thus should provide correct numerical solutions to well-defined boundary value problems. Once the strain energy release rate or stress intensity factor is determined, the onset of brittle fracture can be predicted if the critical values of these quantities are known. Their elastic-plastic extension, the J-integral, has also been used with some success in predicting the onset of ductile fracture. Laws governing other fracture phenomena, such as stable crack growth under large scale yielding, are being investigated through empirical correlations of fracture data with computed fracture parameters.

An approach which has been used recently to establish a stable crack growth criterion is to input actual crack growth data as additional boundary values to an elastic-plastic finite element code. Kanninen et al. [26] used the finite element code in its "generation mode" to study stable crack growth

and instability of A533-B steel and 2219-T87 aluminum center-crack and compact specimens. A similar approach was used by Shih et al. [27] who studied stable crack growth and instability of A533-B compact specimens. Experimentally determined load-line displacement versus crack length relation, as shown in Figure 8, was used to simulate crack extension in the two-dimension finite element model shown in Figure 9. Two sets of elastic-plastic analyses based on J_2 deformation and J_2 flow theories of plasticity were conducted. Figure 10 shows excellent agreements between the measured and computed applied load versus load-line displacement relations obtained by these two numerical analyses. The computed fracture parameters included the crack opening displacement (COD), the crack opening angle (COA), the J-integral and the rate of change of J-integral, dJ/da. Since the fracture criterion for stable crack growth must be independent of specimen geometry and crack extension, these fracture parameters were then scrutinized for constancy during crack extension. Typical dJ/da and COA variations with crack extensions obtained by Shih et al. are shown in Figure 11 and 12, respectively. Both Kaninnen and Shih concluded from their hybrid experimental-numerical investigations that the COA was an attractive fracture criterion for stable crack growth in the presence of large scale yielding.

The above studies demonstrate the utility of the hybrid experimental-numerical technique in extracting candidate fracture parameters which cannot be obtained directly from either the experimental or the numerical analysis alone. The hybrid experimental-numerical technique provided computed fracture parameters, such as J and dJ/da, under actual test conditions and not under assumed test conditions which normally would have been prescribed in pure numerical analysis. The technique also yielded numerically consistent COD and COA which in theory are measurable but in practice are difficult to determine.

The elastic-plastic finite element codes with fracture packages, including those mentioned above, are yet to be subjected to the rigorous scrutiny leveled on the elastic codes. The wide variations in the J-integrals of the mid-1970's [28] hopefully have been reduced if not eliminated in the elasto-plastic finite element codes of today.

DYNAMIC FRACTURE

The state of science on dynamic fracture mechanics studied with dynamic photoelasticity has been presented by J. W. Dally in his 1979 William M. Murray Lecture [29]. He noted that the crack tip state of stress provided by dynamic photoelasticity and dynamic caustic* techniques have and will continue to enhance our understanding on the complex phenomena of dynamic crack propagation. Dynamic fracture studies by these techniques, however, are limited to photoelastic polymers and to plane stress problems when photoelastic coatings or caustics are used. The hybrid experimental-numerical technique, when used with the generation mode of finite element or finite difference method will extract dynamic fracture parameters in opaque materials as well as in non-plane stress problems. These dynamic codes which, unlike the well-studied static codes, required verificaion prior to its used in dynamic fracture mechanics. Fracture dynamic results generated by various two-dimensional elasto-dynamic finite difference codes [30,31] and finite element codes [32,33] have been compared with dynamic caustic results of fracturing polymeric specimens [34,35]. Similar verification studies have been conducted with dynamic photoelasticity [36].

The verified numerical code can also be used to check ancillary results

---

*Added by the author.

deduced from the original experimental results, such as the variation in input work, which cannot be easily measured, during the fracture process. Numerical analysis also provides the transient energy partition for the input boundary and initial conditions. Such energy partition can then be used to check the hypothesis used in deducing the experimentally determined energy partition. The legend of Figure 13 shows an internally notched, semicircular photoelastic specimen which was loaded with end rotation and shear deformation [37]. The reported dynamic fracture toughness versus crack velocity relation [29] was used as a dyanmic fracture criterion to execute a dynamic finite element code in its application mode which yielded the crack propagation and dynamic stress intensity factor histories [38] which are in good agreement with the numerical results. Having verified the numerical modeling of the photoelastic experiment, the energies during crack propagation were computed and plotted as shown in Figure 14. The internal consistency in the computed energy partition verifies the basic postulates of negligible viscoelastic damping and negligible energy dissipation at the finite specimen boundaries during the dynamic crack propagation period.

A relatively simple application of the hybrid technique is the determination of the dynamic stress intensity factor in an impacted notch bend specimen. Measured time variations in the striker load were input to the finite element model of a dynamic finite element code which was then used to compute the time variations in the dynamic stress intensity factor [40]. The numerical code was also verified by comparing the computed and measured dynamic strains near the crack tip as shown in Figure 15. Figure 16 shows the variations in dynamic and the corresponding static stress intensity factors with time prior to the crack propagation. These results show the inadequacy of the static stress intensity factor which was computed by using a static formula

and the instantaneous striker load. It also indicates the futility in interpreting such impact fracture response without the use of proper dynamic analysis [41]. As a verification of codes, Figure 17 shows the agreement between three independent dynamic fracture analyses of another impacted three point bend specimen [42].

Figure 18 shows a wedge loaded, modified-tapered double cantilever beam (WL-MTDCB) specimen which was fabricated from plate glass. The specimen was 25% side-grooved to guide the propagating crack. The flexible, long tapered beam sections was designed to lessen the friction with the silicon carbide loading pin. The specimen was wedge-loaded to fracture in a 500-kg Instron testing machine and the crack extension history was recorded by a KRAK-GAGE and associated instrumentation [43]. Figure 19 shows typical crack length versus time data which is characterized by the unambiguous initial period of crack acceleration and which has not been observed in dynamic fracture of metals and photoelastic polymers. The average of the two data sets, which is represented by a solid curve in Figure 19, was used to drive a dynamic finite element code in its generation mode. The resultant K_I^{dyn} as well as the static stress intensity factor, K_I^{stat}, which was also computed by finite element analysis, are shown in Figure 20. Although it is not obvious from Figure 20, unlike the dynamic fracture of metals and polymers, the crack never arrested in these and other ceramics WL-MTDCB specimens [40]. Thus the K_I^{dyn} versus a curve in Figure 21 should continue past the nominal static fracture toughness K_{IC} = 0.73 Mpa m as indicated by the dashed lines. Notable is the lack of the typical gamma-shaped K_I^{dyn} versus a commonly observe in metals and polymers.

CONCLUSION

The hybrid experimental-numerical technique yields reliable information which cannot be obtained by the single use of either the experimental or numerical technique. The utility of the hybrid experimental-numerical technique in experimental mechanics is demonstrated by case studies in two- and three-dimensional stress analysis, biomechanics and fracture mechanics.

ACKNOWLEDGEMENTS

This Murray Lecture is the ultimate in one's professional career, which I owe to my mentors, Emmett E. Day and August J. Durelli, who taught me the science as well as the difficult art of experimental stress analysis and Paul R. Trumpler, who initiated me into numerical structural analysis. I am indebted to my colleagues, James W. Dally, William F. Riley, Paul C. Paris, Charles F. Tiffany, Michael E. Fourney, Ashley F. Emery, Satya N. Atluri, Takeshi Kanazawa, James I. Mueller and Neil M. Hawkins, whose ideas and encouragement strongly influenced my career, to my home institutions, Illinois Institute of Technology and the University of Washington and the respective faculty and staff, whose names are too numerous to list here, and to my past and present funding agencies, ONR, NSF, ARO, NIH, AFOSR, DOT and NASA. Last, but not the least, I wish to acknowledge the efforts of my former and present graduate students who are the real heroes in the often frustrating experimental and numerical analyses.

REFERENCES

1. Durelli, A. J., Applied Stress Analysis, Prentice-Hall Inc., Englewood Cliffs, NJ, 1967, p.6.

2. Dally, J. W. and Riley, W. F., Experimental Stress Analysis, McGraw Hill, 1978, pp. 459-467.

3. Lee, G. H., An Introduction to Experimental Stress Analysis, John Wiley & Sons, New York, 1950, pp. 202-208.

4. Frocht, M. M., Photoelasticity, John Wiley & Sons, New York, Vol. 2, 1948, pp. 238-332.

5. Frocht, M. M., Photoelasticity, John Wiley & Sons, New York, Vol. 1, 1941, pp. 252-286.

6. Coker, E. G. and Filon, L. N. G., A Treaties on Photoelasticity, Cambridge University Press, London, 1931, pp. 143-145.

7. Durelli, A. J. and Riley, W. F., Introduction to Photomechanics, Prentice-Hall, Englewood Cliffs, 1965, pp. 185-186.

8. Rao, G. V., "Experimental-numerical Hybrid Techniques for Body-force and Thermal Stress Problems - Applications in Power Industry", Proc. of the 1982 Joint Conference on Experimental Mechanics, SESA, 1982, pp. 398 - 404.

9. Barishpolsky, B. M., "A Combined Experimental and Numerical Method for the Solution of Generalized Elasticity Problem", Experimental Mechanics, Vol. 20, Oct. 1980, pp. 345 - 349.

10. Barishpolsky, B. M., "Development of a Combined Experimental and Numerical Method for the Thermoelastic Analysis", Proc. of 1981 SESA Spring Meeting, 1981.

11. Moslehy, F. A. and Ranson, W. F., "Laser Speckle Interferometry and Boundary Integral Techniques in Experimental Stress Analysis", Developments Theoretical and Applied Mechanics, Vol. X, ed. by J. E. Stoneking, The University of Tennessee, 1980, pp. 473 - 492.

12. Balas, J., Sladek, J. and Drzik, M., "Stress-analysis by Combination of Holographic Interferometry and Boundary Integral Method", to be published in Experimental Mechanics.

13. Umeagukwu, I., Peters, W. and Ranson, W. F., "The Experimental Boundary Integral Method in Photoelasticity", Developments in Theoretical and Applied Mechanics, Vol. XI. edt. by T. J. Chung and G. R. Karr, The University of Alabama in Huntsville, 1982, pp. 181 - 191.

14. Collins, R. and van der Werff, T., Mathematical Models of the Dynamics of the Human Eye, Springer-Verlag, Berlin, 1980, p. 1.

15. Enoch, J. M., "Causes and Costs of Visual Impairment", Vision and Its Disorders, NINDB Monograph No. 4, HEW, 1967, pp. 23 -28.

16. Friedenwald, J. S., "Contribution to the Theory and Practice of Tonometry", American Journal of Ophthalmology, Vol. 20, 1937, pp. 985 - 1024.

17. Nyquist, G. N., "Rheology of the Cornea: Experimental Techniques and Results", Experimental Eye Research, Vol. 7, 1968, pp. 183 - 188.

18. Gloster, J., Perkins, E. S. and Pommier, M., "Extensibility of Strips of Sclera and Cornea", Brit. J. of Ophthalmology, Vol. 41, 1957, pp. 103 -

110.

19. Woo, S., Kobayashi, A. S., Schlegel, W. A. and Lawrence, C., "Nonlinear Material Properties of Intact Cornea and Sclera", Experimental Eye Research, Vol. 14, 1972, pp. 29 - 39.

20. Woo, S., Kobayashi, A. S., Schlegel, W. A. and Lawrence, C., "Mathematical Model of the Corneo-Scleral Shell as Applied to Pressure-Volume Relations and Applanation Tonometry", Annals of Biomedical Engineering, Vol. 1, Sept. 1972, pp. 87 -98.

21. St. Helen, R. and McEwen, W. K., "Rheology fo the Human Eye", Amer. J. of Ophthalmology, Vol. 51, 1961, pp. 539 - 548.

22. Kobayashi, A. S., Brown, C. A., and Emery, A.F., "Viscoelastic Response of the Corneo-Sclera Shell Under Tonometer Loading", ASME Preprint 75-WA/Bio-2, 1975.

23. Drucker, D. C., "Thoughts on the Present and Future Interrelation of Theoretical and Experimental Mechanics", Experimental Mechanics, Vol. 8, Mar. 1968, pp. 97 - 106.

24. Gloster, J., "Tonometry and Tonography", International Ophthalmology Clinics, Vol. 5, 1965.

25. "A Critical Evaluation of Numerical Solutions to the 'Benchmark' Surface Flaw Problem", ed. by J. J. McGowan, Soc. for Experimental Stress Analysis, 1980.

26. Kanninen, M. F., Rybicki, E. F., Stonesifer, R. B., Broek, D., Rosenfield, A. R., Marschall, C. W. and Hahn, G. T., "Elastic-Plastic Fracture Mechanics for Two-Dimensional Stable Crack Growth and Instability Problems", Elastic-Plastic Fracture, ed. by J. D. Landes, J. A. Begley and G. A. Clarke, ASTM STP 668, 1979, pp. 121 -150.

27. Shih, C. F., deLorenzi, H. G. and Andrews, W. R., " Studies on Crack Initiation and Stable Crack Growth", Elastic-Plastic Fracture, ed. by J. D. Landes, J. A. Begley and G. A. Clarke, ASTM STP 668, 1979, pp. 65 - 120.

28. Wilson, W. K., and Osias, J. R., "A Comparison of Finite Element Solutions for an Elastic-Plastic Problem", Int. J. of Fracture, Vol. 14, 1978, pp. R95 - 108.

29. Dally. J. W., "Dynamic Photoelastic Studies of Fracture", Experimental Mechanics, Vol. 19, 1979, pp. 349 - 361.

30. Shmuely, M. and Perl, M., "The SMF2D Code for Proper Simulation of Crack Propagation", Crack Arrest Methodology and Applications, ed. by G. T. Hahn and M. F. Kanninen, ASTM STP 711, 1980, pp. 54 - 69.

31. Popelar, C. H. and Gehlen, P. C., "Modeling of Dynamic Crack Propagation: II. Validation of Dynamic Analysis", Int. J. of Fracture, Vol. 15, 1979,

pp 159 - 177.

32. Hodulak, L., Kobayashi, A. S. and Emery, A. F., "A Crtical Examination of a Numerical Fracture Dynamic Code", Fracture Mechanics, ed. by P. C. Paris, ASTM STP 700, 1980, pp. 174 - 188.

33. Nishioka, T. and Atluri, S. N., "Numerical Analysis of Dynamic Crack Propagation: Generation and Prediction Studies", Engineering Fracture Mechanics, Vol. 16, No. 3, 1982, pp. 303-332.

34. Kalthoff, J. F., Beinert, J. and Winkler, S., "MeasurementBs of Dynamic Stress Intensity Factors for Fast Running and Arresting Cracks in Double Cantilever-Beam Specimens", Fast Fracture and Crack Arrest, ed. by G. T. Hahn and M. F. Kanninen, ASTM STP 627, 1977, pp. 161 -176.

35. Kalthoff, J. F., Beinert, J. and Winkler, S., "Influence of Dynamic Effects on Crack Arrest", Institut fur Festkorpemechanik, EPRI RP 1022-1, IKFM 404012, August 1978.

36. Kobayashi, A. S., Seo, K., Jou, J.-Y. and Urabe, Y., "Dynamic Analysis of Homalite -100 and Polycarbonate Modified Compact tension Specimens", Experimental Mechanics, Vol. 20, Sept. 1980, pp. 73 -79.

37. Dally, J. W., Shukla, A. and Kobayashi, T., "A Dynamic Photoelastic Study of Crack Propagation in a Ring Specimen", Crack Arrest Methodology and Applications, ed. by G. T. Hahn and M. F. Kanninen, ASTM STP 711, June 1980, pp. 161 - 177.

38. Kobayashi, A. S., Emery, A. F. and Liaw, B.-M., "Dynamic Fracture of Three Specimens", to be published in Fracture Mechanics, ASTM STP.

39. Shukla, A. and Dally, J. W., "A Photoelastic Study of Energy Loss During A Fracture Event", Experimental Mechanics, Vol. 21, April 1981, pp. 163 - 168.

40. Mall, S., Kobayashi, A. S. and Loss, F. J.,"Dyanmic Fracture Analysis of Notch Bend Specimen", Crack Arrest Methodology and Applications, ed. by G. T. Hahn and M. F. Kanninen, ASTM STP 711, 1980, pp. 70 -85.

41. Kobayashi, A. S., Ramulu, M. and Mall, S., "Impacted Notch Bend Specimens", ASME J. of Pressure Vessel Technology, Vol. 104, Feb. 1982, pp. 25 - 30.

42. Kobayashi, A. S., "Numerical Analysis in Fracture Mechanics", to be published in the Proc. of the International Conference on Application of Fracture Mechanics to Materials and Structures, Freiburg, Germany, June 1983.

43. Kobayashi, A. S., Emery, A. F. and Liaw, B.-M., "Dynamic Fracture Toughness of Glass", to be published in the Proceedings of the International Symposium on Fracture Mechanics of Ceramics, Plenum Press, 1983.

44. Kobayashi, A. S., Emery, A. F. and Liaw, B. M., "Dynamic Fracture Toughness of Reaction Bonded Silicon Nitride", J. of American Society,

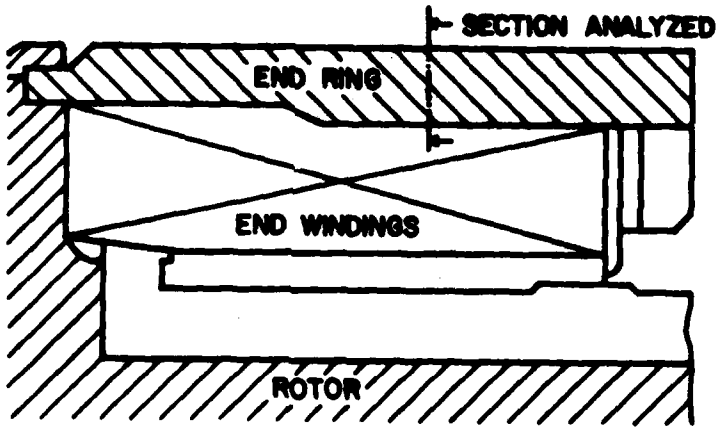

Fig. 1a End Ring Assembly on Rotor

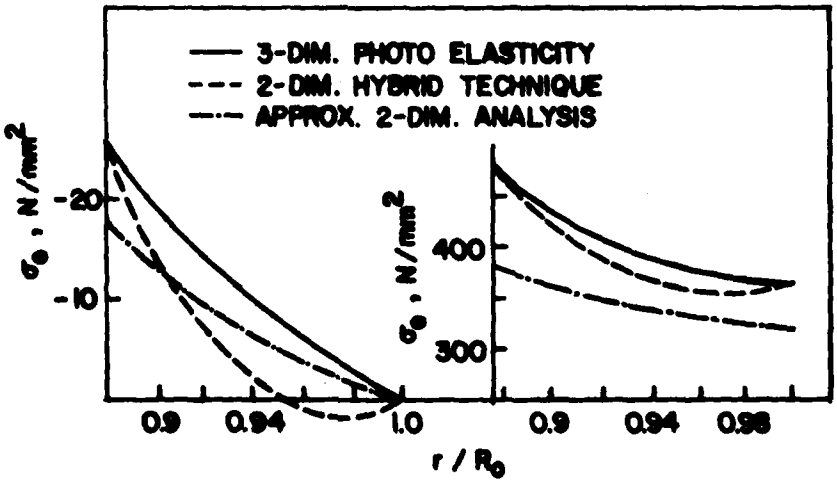

Fig. 1b Hoop Stress in End Ring Due to Centrifugal Forces

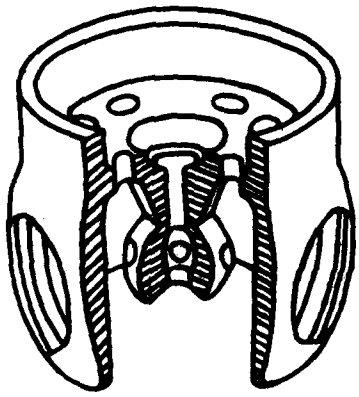

Fig. 2a The Model of the Working Wheel of a Water Turbine

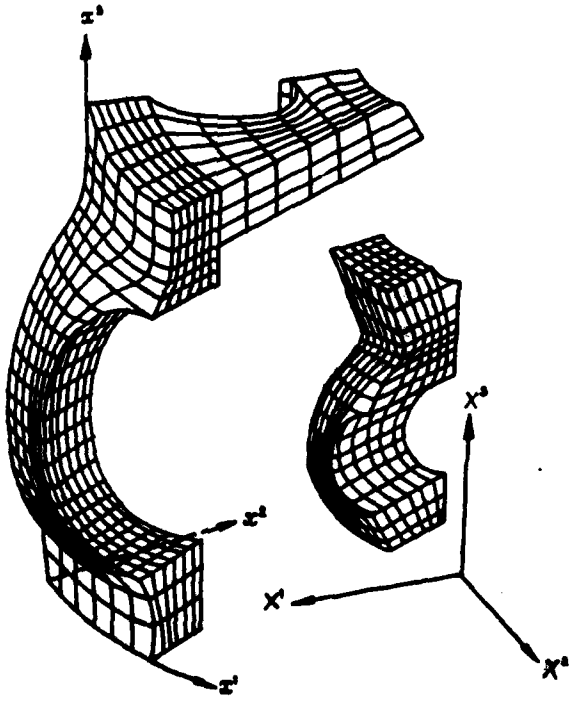

Fig. 2b Finite Difference Network

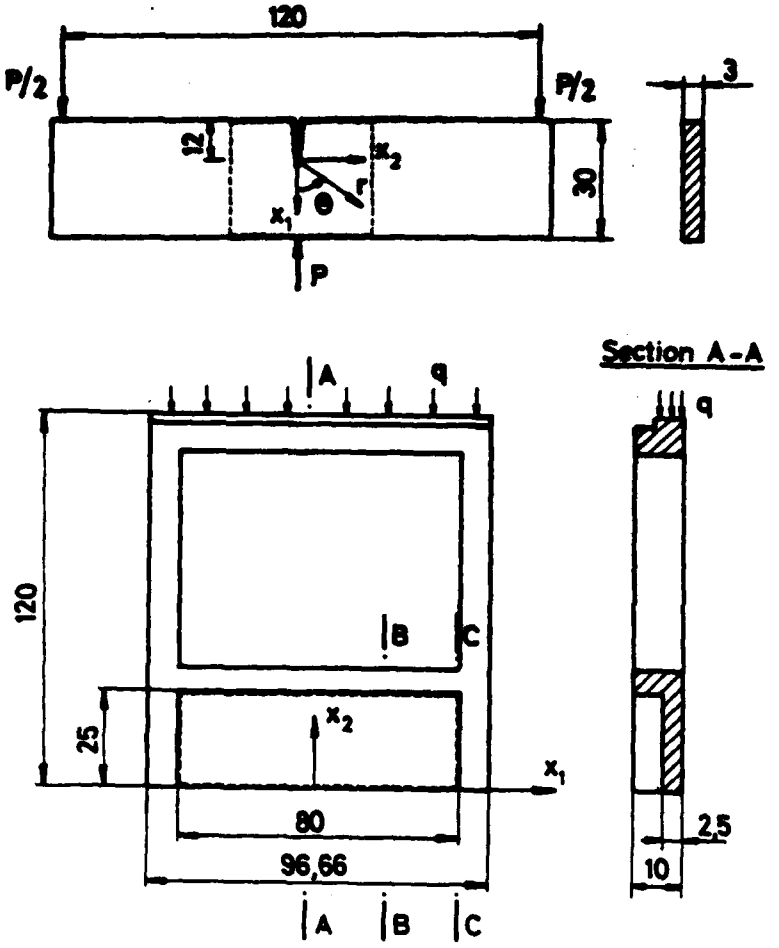

Fig. 3 Plate-Stiffened Frame

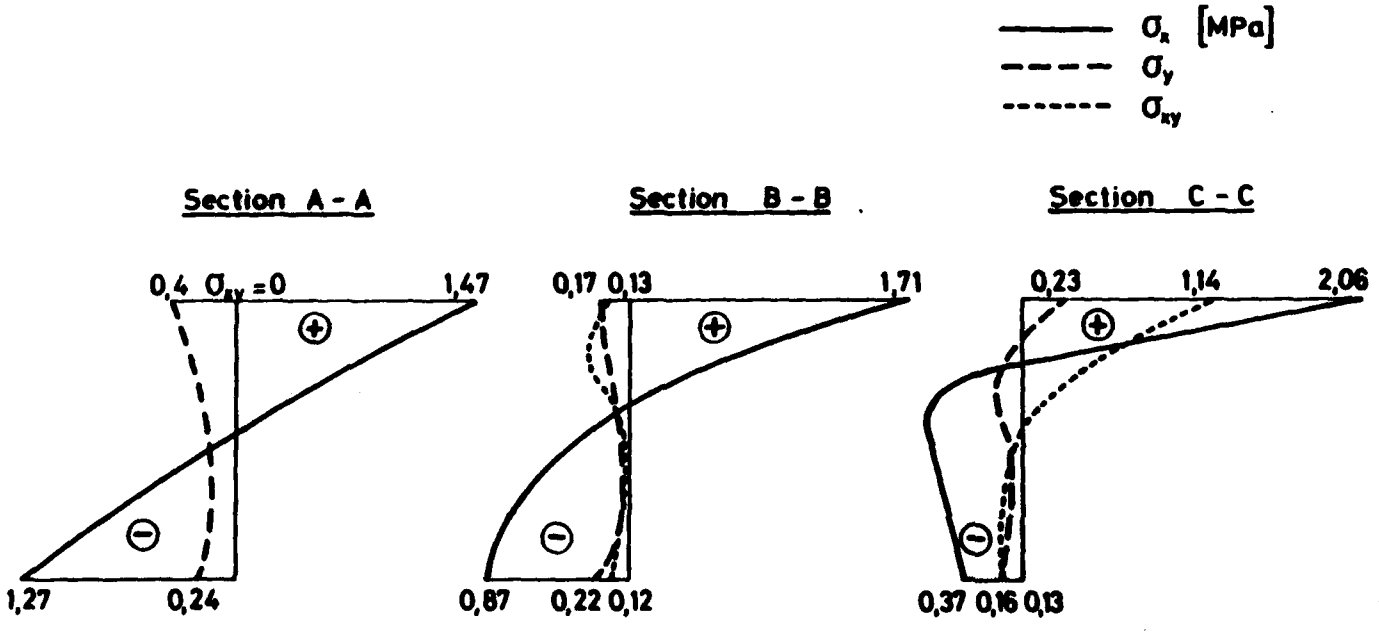

Fig. 4 Stresses in Plate Stiffened Frame

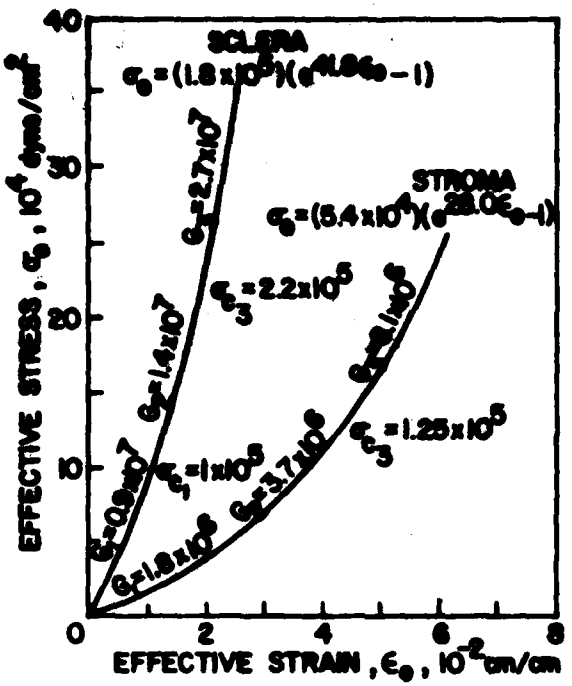

Fig. 5 Trilinear and Experimental Stress-Strain Relation

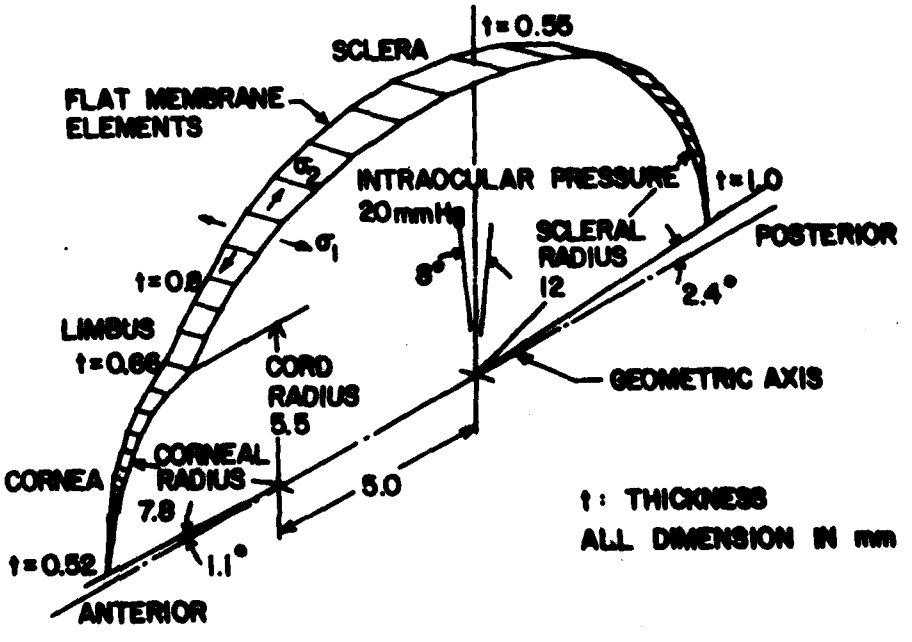

Fig. 6 Membrane Model Finite Element Arrangement

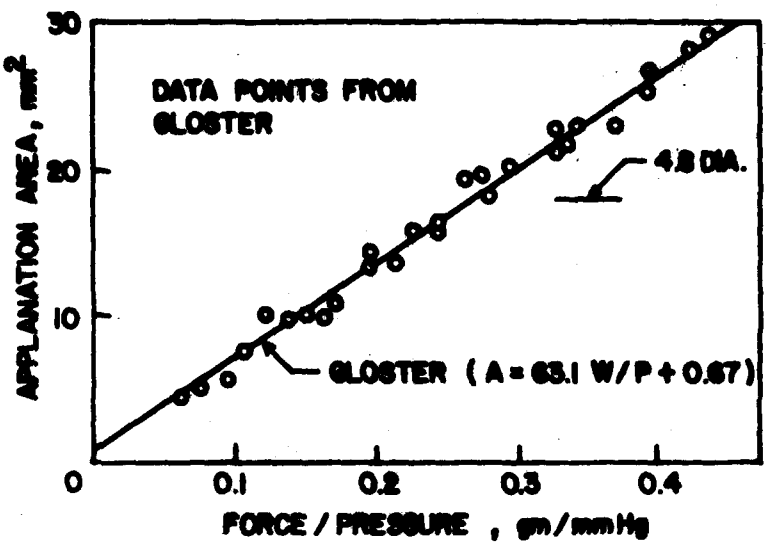

Fig. 7 Applanation Force/Intraocular Pressure vs Applanation Area

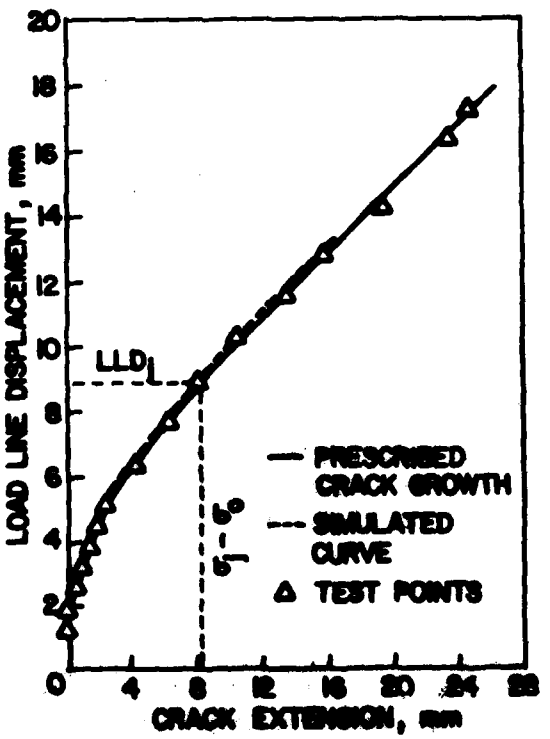

Fig. 8 Prescribed and Simulated Load-Line Displacement vs Crack Extension for 4T Compact Specimen

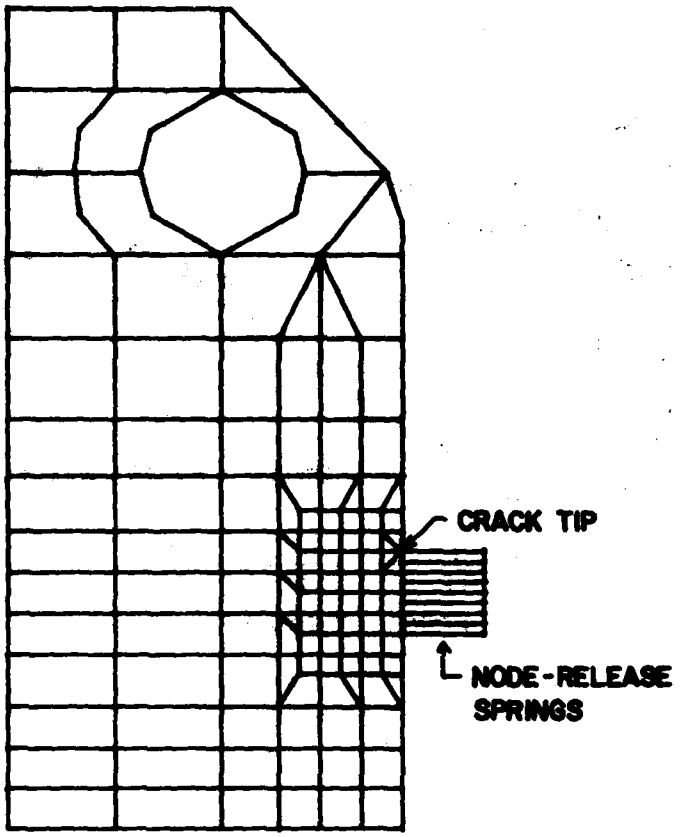

Fig. 9 Finite-Element Model for 4T Compact Specimen

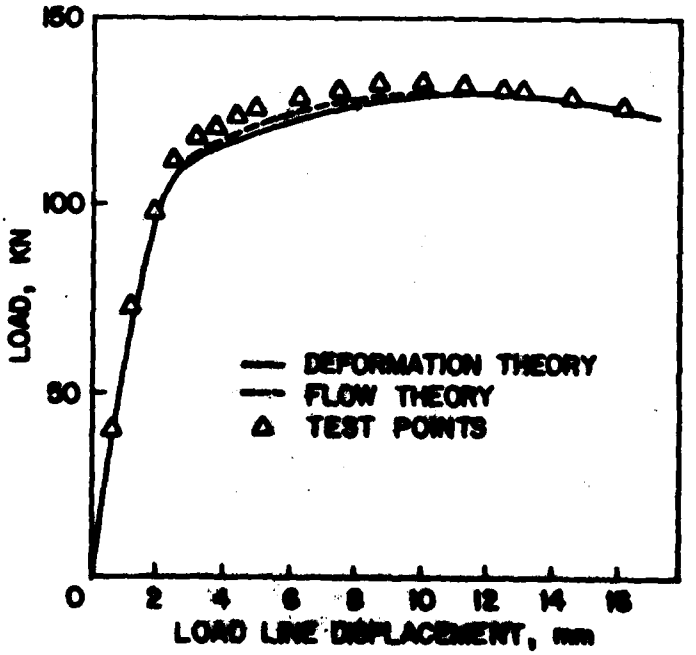

Fig. 10 Applied Load vs Load-Line Displacement for 4T Compact Specimen, 25% Side-Grooved, $W-a_o$ = 40 mm (1.593 in.)

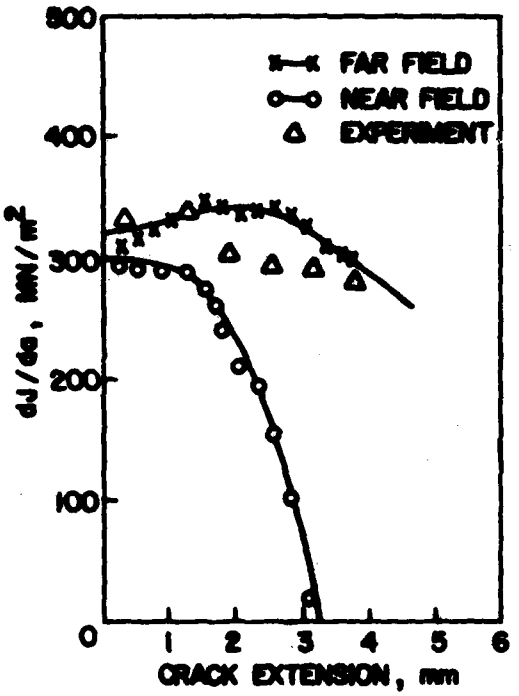

Fig. 11 dJ/da for Compact Specimen T-61, a/W = 0.801

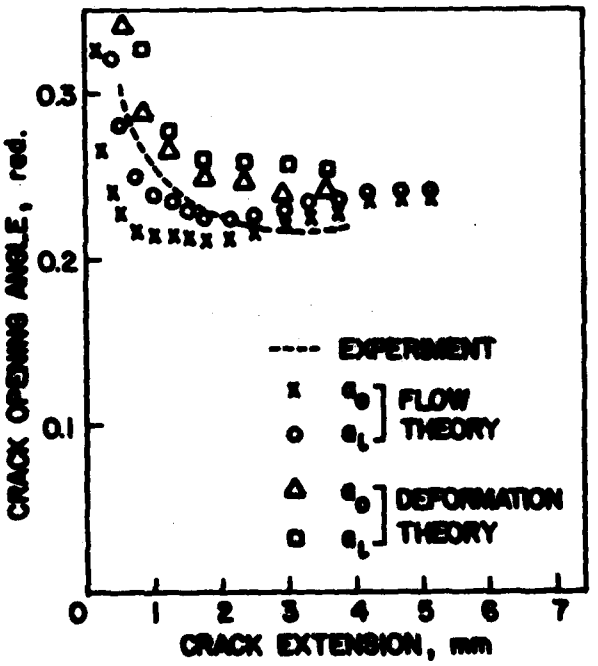

Fig. 12 Crack-Opening Angle vs Crack Extension for 4T Compact Specimen

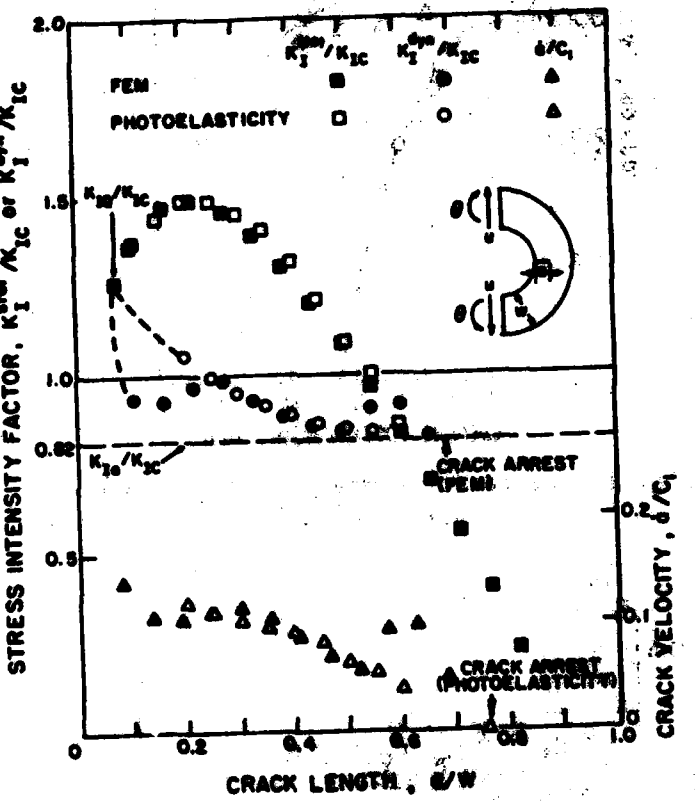

Fig. 13 Stress Intensity Factors and Crack Velocities of Internally Notched Semi-Circular Homalite-100 Specimen Subjected to End Rotation and Shear Formation

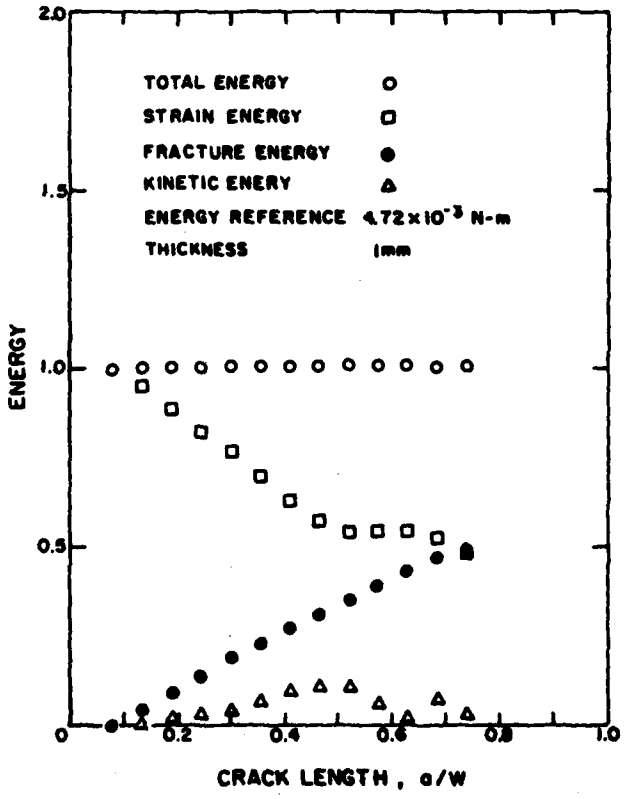

Fig. 14 Energies in Internally Notched, Semi-Circular Homalite-100 Specimen Subjected to End Rotation and Shear Deformation

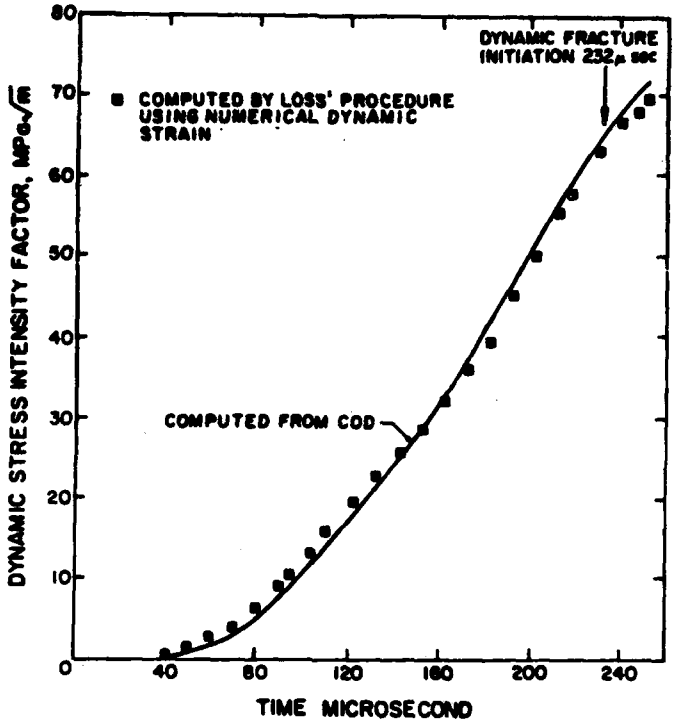

Fig. 15 Dynamic Strain at Location (1), A533B Bend Specimen

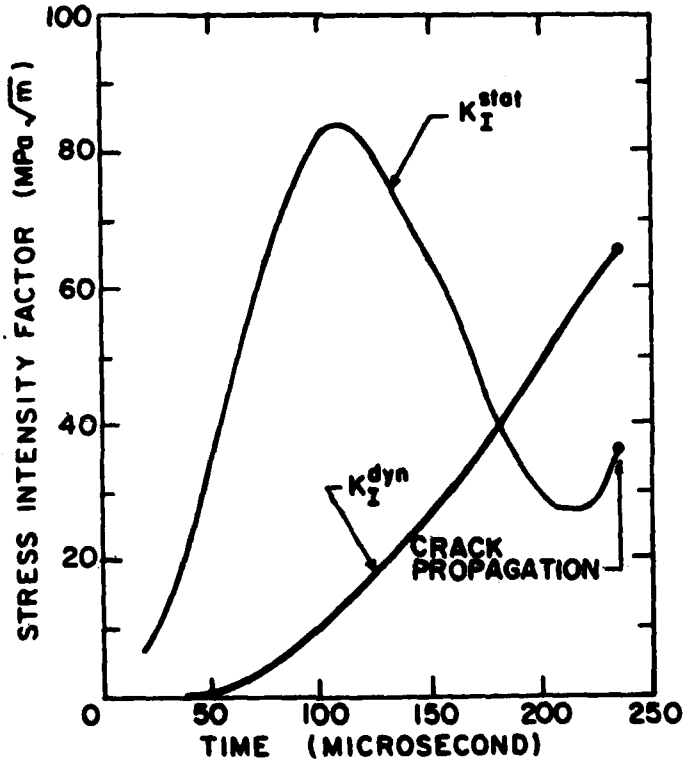

Fig. 16 Stress Intensity Factors of an Impacted A533B Steel Notched Bend Specimen (L = 229, W=51, B=25, a=25mm)

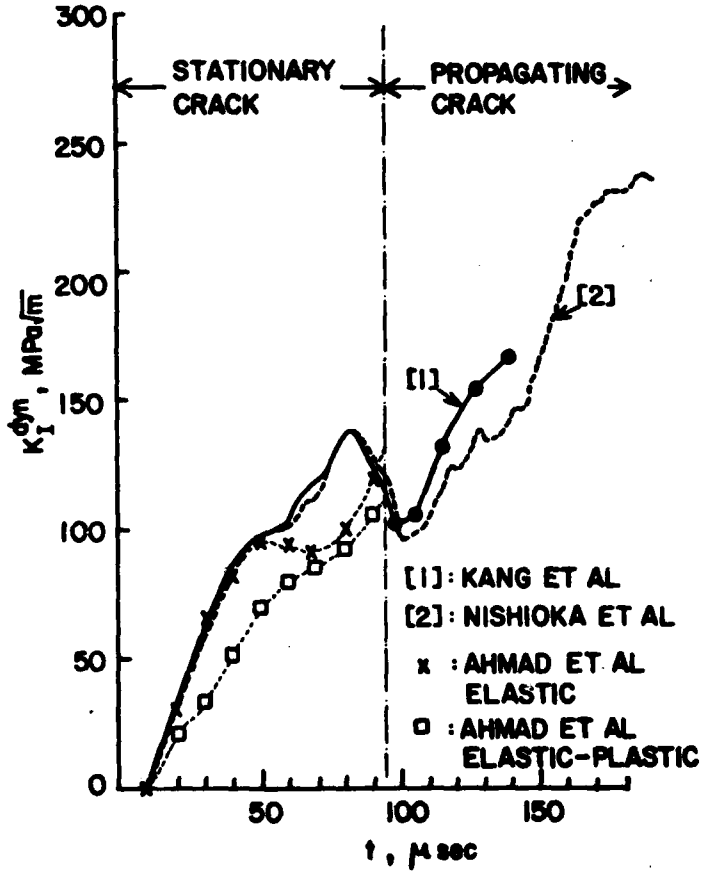

Fig. 17 Dynamic Stress Intensity Factor of a Dynamic Tear Test Specimen

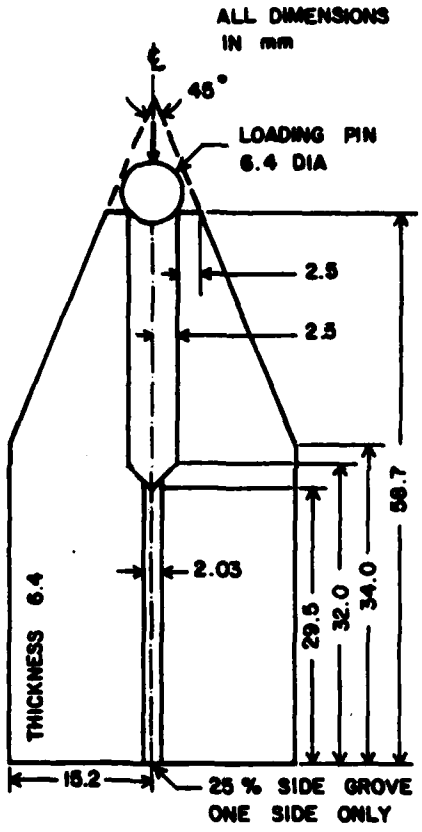

Fig. 18 Glass WL-MTDCB Specimen

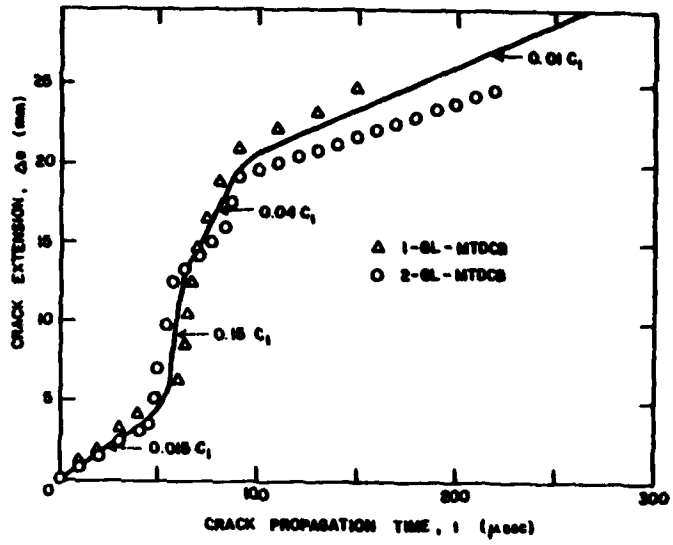

Fig. 19 Crack Extension vs Time of Fracturing WL-MTDCB Glass Specimen

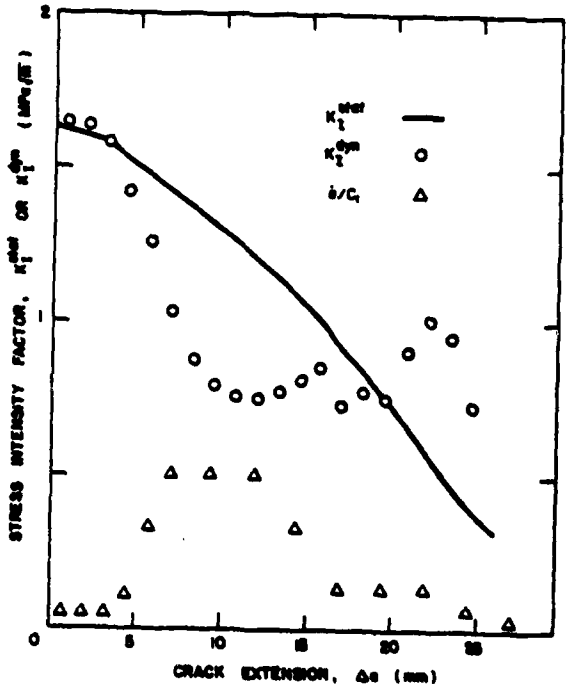

Fig. 20 Stress Intensity Factors and Crack Velocities in a Fracturing WL-MTDCB Glass Specimen

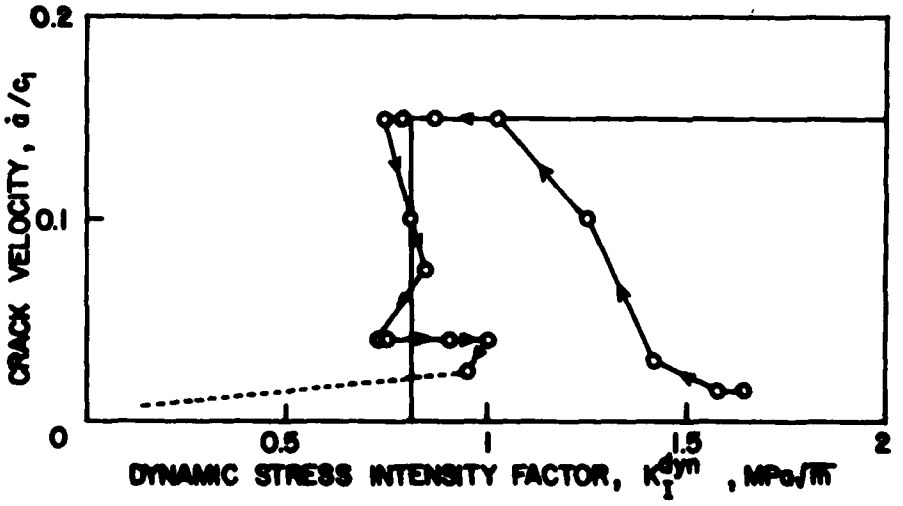

Fig. 21 Dynamic Fracture Toughness vs Crack Velocity Relation for Glass

474:MP:716:lab
78s474-619

Part 1 - Government

Administrative and Liaison Activities

Office of Naval Research
Department of the Navy
Arlington, VA 22217
Attn: Code 474 (2)
471
200

Director
Office of Naval Research
Branch Office
666 Summer Street
Boston, MA 02210

Director
Office of Naval Research
Branch Office
536 South Clark Street
Chicago, IL 60605

Director
Office of Naval Research
Branch Office
1030 East Green Street
Pasadena, CA 91106

Naval Research Laboratory (6)
Code 2627
Washington, D.C. 20375

Defense Documentation Center (12)
Cameron Station
Alexandria, Virginia 22314

Navy

Underseas Explosion Research Division
Naval Ship Research and Development Center
Norfolk Naval Shipyard
Portsmouth, VA 23709
Attn: Dr. E. Palmer, Code 177

Navy (Con't.)

Naval Research Laboratory
Washington, D.C. 20375
Attn: Code 8400
8410
8430
8440
6300
6390
6380

David W. Taylor Naval Ship Research and Development Center
Annapolis, MD 21402
Attn: Code 2740
28
281

Naval Weapons Center
China Lake, CA 93555
Attn: Code 4062
4520

Commanding Officer
Naval Civil Engineering Laboratory
Code L31
Port Hueneme, CA 93041

Naval Surface Weapons Center
White Oak
Silver Spring, MD 20910
Attn: Code R-10
G-402
K-82

Technical Director
Naval Ocean Systems Center
San Diego, CA 92152

Navy Underwater Sound
Reference Division
Naval Research Laboratory
P.O. Box 8337
Orlando, FL 32806

Navy (Con't.)

Chief of Naval Operations
Department of the Navy
Washington, D.C. 20350
Attn: Code OP-098

Strategic Systems Project Office
Department of the Navy
Washington, D.C. 20376
Attn: NSP-200

Naval Air Systems Command
Department of the Navy
Washington, D.C. 20361
Attn: Code 5302 (Aerospace and Structures)
604 (Technical Library)
320R (Structures)

Naval Air Development Center
Warminster, PA 18974
Attn: Aerospace Mechanics
Code 606

U.S. Naval Academy
Engineering Department
Annapolis, MD 21402

Naval Facilities Engineering Command
200 Stovall Street
Alexandria, VA 22332
Attn.: Code 03 (Research & Development)
04B
045
14114 (Technical Library)

Naval Sea Systems Command
Department of the Navy
Washington, D.C. 20362
Attn: Code 05H
312
322
323
05R
32R

Navy (Con't.)

Commander and Director
David W. Taylor Naval Ship Research and Development Center
Bethesda, MD 20084
Attn: Code 042
17
172
173
174
1800
1844
012.2
1900
1901
1945
1960
1962

Naval Underwater Systems Center
Newport, RI 02840
Attn: Dr. R. Trainor

Naval Surface Weapons Center
Dahlgren Laboratory
Dahlgren, VA 22448
Attn: Code G04
G20

Technical Director
Mare Island Naval Shipyard
Vallejo, CA 94592

U.S. Naval Postgraduate School
Library
Code 0384
Monterey, CA 93940

Webb Institute of Naval Architecture
Attn: Librarian
Crescent Beach Road, Glen Cove
Long Island, NY 11542

Army

Commanding Officer (2)
U.S. Army Research Office
P.O. Box 12211
Research Triangle Park, NC 27709
Attn: Mr. J. J. Murray, CRD-AA-IP

474:MP:716:lab
78s474-619

Army (Con't.)

Watervliet Arsenal
MAGGS Research Center
Watervliet, NY 12189
Attn: Director of Research

U.S. Army Materials and Mechanics Research Center
Watertown, MA 02172
Attn: Dr. R. Shea, DRXMR-T

U.S. Army Missile Research and Development Center
Redstone Scientific Information Center
Chief, Document Section
Redstone Arsenal, AL 35809

Army Research and Development Center
Fort Belvoir, VA 22060

NASA

National Aeronautics and Space Administration
Structures Research Division
Langley Research Center
Langley Station
Hampton, VA 23365

National Aeronautics and Space Administration
Associate Administrator for Advanced
Washington, D.C. 20546

Air Force

Wright-Patterson Air Force Base
Dayton, OH 45433
Attn: AFFDL (FY)
(FBR)
(FBE)
(FBS)
AFML (MBM)

474:MP:716:lab
78s474-619

Air Force (Con't.)

Chief Applied Mechanics Group
U.S. Air Force Institute of Technology
Wright-Patterson Air Force Base
Dayton, OH 45433

Chief, Civil Engineering Branch
WLRC, Research Division
Air Force Weapons Laboratory
Kirtland Air Force Base
Albuquerque, NM 87117

Air Force Office of Scientific Research
Bolling Air Force Base
Washington, D.C. 20332
Attn: Mechanics Division

Department of the Air Force
Air University Library
Maxwell Air Force Base
Montgomery, AL 36112

Other Government Activities

Commandant
Chief, Testing and Development Division
U.S. Coast Guard
1300 E Street, NW.
Washington, D.C. 20226

Technical Director
Marine Corps Development and Education Command
Quantico, VA 22134

Director Defense Research and Engineering
Technical Library
Room 3C128
The Pentagon
Washington, D.C. 20301

Other Government Activities (Con't.)

Dr. H. Gaus
National Science Foundation
Environmental Research Division
Washington, D.C. 20550

Library of Congress
Science and Technology Division
Washington, D.C. 20540

Director
Defense Nuclear Agency
Washington, D.C. 20305
Attn: SPSS

Mr. Jerome Persh
Staff Specialist for Materials and Structures
OUSDR&E, The Pentagon
Room 3D1089
Washington, D.C. 20301

Chief, Airframe and Equipment Branch
FS-120
Office of Flight Standards
Federal Aviation Agency
Washington, D.C. 20553

National Academy of Sciences
National Research Council
Ship Hull Research Committee
2101 Constitution Avenue
Washington, D.C. 20418
Attn: Mr. A. R. Lytle

National Science Foundation
Engineering Mechanics Section
Division of Engineering
Washington, D.C. 20550

Picatinny Arsenal
Plastics Technical Evaluation Center
Attn: Technical Information Section
Dover, NJ 07810

Maritime Administration
Office of Maritime Technology
14th and Constitution Ave., NW.
Washington, D.C. 20230

474:MP:716:lab
78s474-619

PART 2 - Contractors and other Technical Collaborators

Universities

Dr. J. Tinsley Oden
University of Texas at Austin
345 Engineering Science Building
Austin, TX 78712

Professor Julius Miklowitz
California Institute of Technology
Division of Engineering and Applied Sciences
Pasadena, CA 91109

Dr. Harold Liebowitz, Dean
School of Engineering and Applied Science
George Washington University
Washington, D.C. 20052

Professor Eli Sternberg
California Institute of Technology
Division of Engineering and Applied Sciences
Pasadena, CA 91109

Professor Paul M. Naghdi
University of California
Department of Mechanical Engineering
Berkeley, CA 94720

Professor A. J. Durelli
Oakland University
School of Engineering
Rochester, MD 48063

Professor F. L. DiMaggio
Columbia University
Department of Civil Engineering
New York, NY 10027

Professor Norman Jones
The University of Liverpool
Department of Mechanical Engineering
P.O. Box 147
Brownlow Hill
Liverpool L69 3BX
England

Professor R. J. Hendrych
Pennsylvania State University
Applied Research Laboratory
Department of Physics
State College, PA 16801

Universities (Con't.)

Professor J. Klosner
Polytechnic Institute of New York
Department of Mechanical and Aerospace Engineering
333 Jay Street
Brooklyn, NY 11201

Prof. R. A. Schapery
Texas A&M University
Department of Civil Engineering
College Station, TX 77843

Professor Walter D. Pilkey
University of Virginia
Research Laboratories for the Engineering Sciences and Applied Sciences
Charlottesville, VA 22901

Professor K. D. Willmert
Clarkson College of Technology
Department of Mechanical Engineering
Potsdam, NY 13676

Dr. Walter E. Haisler
Texas A&M University
Aerospace Engineering Department
College Station, TX 77843

Dr. Hussein A. Kamel
University of Arizona
Department of Aerospace and Mechanical Engineering
Tucson, AZ 85721

Dr. S. J. Fenves
Carnegie-Mellon University
Department of Civil Engineering
Schenley Park
Pittsburgh, PA 15213

Dr. Ronald L. Huston
Department of Engineering Analysis
University of Cincinnati
Cincinnati, OH 45221

Universities (Con't.)

Professor G. C. M. Sih
Lehigh University
Institute of Fracture and Solid Mechanics
Bethlehem, PA 18015

Professor Albert S. Kobayashi
University of Washington
Department of Mechanical Engineering
Seattle, WA 98105

Professor Daniel Frederick
Virginia Polytechnic Institute and State University
Department of Engineering Mechanics
Blacksburg, VA 24061

Professor A. C. Eringen
Princeton University
Department of Aerospace and Mechanical Sciences
Princeton, NJ 08540

Professor E. H. Lee
Stanford University
Division of Engineering Mechanics
Stanford, CA 94305

Professor Albert I. King
Wayne State University
Biomechanics Research Center
Detroit, MI 48202

Dr. V. R. Hodgson
Wayne State University
School of Medicine
Detroit, MI 48202

Dean B. A. Boley
Northwestern University
Department of Civil Engineering
Evanston, IL 60201

Universities (Con't.)

Professor P. G. Hodge, Jr.
University of Minnesota
Department of Aerospace Engineering and Mechanics
Minneapolis, MN 55455

Dr. D. C. Drucker
University of Illinois
Dean of Engineering
Urbana, IL 61801

Professor N. J. Newmark
University of Illinois
Department of Civil Engineering
Urbana, IL 61803

Professor E. Reissner
University of California, San Diego
Department of Applied Mechanics
La Jolla, CA 92037

Professor William A. Nash
University of Massachusetts
Department of Mechanics and Aerospace Engineering
Amherst, MA 01002

Professor G. Herrmann
Stanford University
Department of Applied Mechanics
Stanford, CA 94305

Professor J. D. Achenbach
Northwest University
Department of Civil Engineering
Evanston, IL 60201

Professor S. B. Dong
University of California
Department of Mechanics
Los Angeles, CA 90024

Professor Burt Paul
University of Pennsylvania
Towne School of Civil and Mechanical Engineering
Philadelphia, PA 19104

Universities (Con't.)

Professor H. W. Liu
Syracuse University
Department of Chemical Engineering and Metallurgy
Syracuse, NY 13210

Professor S. Bodner
Technion R&D Foundation
Haifa, Israel

Professor Werner Goldsmith
University of California
Department of Mechanical Engineering
Berkeley, CA 94720

Professor R. S. Rivlin
Lehigh University
Center for Application of Mathematics
Bethlehem, PA 18015

Professor F. A. Cozzarelli
State University of New York at Buffalo
Division of Interdisciplinary Studies
Karr Parker Engineering Building
Chemistry Road
Buffalo, NY 1[illegible]14

Professor Joseph [illegible]. Rose
Drexel University
Department of Mechanical Engineering and Mechanics
Philadelphia, PA 19104

Professor B. K. Donaldson
University of Maryland
Aerospace Engineering Department
College Park, MD 20742

Professor Joseph A. Clark
Catholic University of America
Department of Mechanical Engineering
Washington, D.C. 20064

Universities (Con't.)

Dr. Samuel B. Batdorf
University of California
School of Engineering and Applied Science
Los Angeles, CA 90024

Professor Isaac Fried
Boston University
Department of Mathematics
Boston, MA 02215

Professor E. Krempl
Rensselaer Polytechnic Institute
Division of Engineering
Engineering Mechanics
Troy, NY 12181

Dr. Jack R. Vinson
University of Delaware
Department of Mechanical and Aerospace Engineering and the Center for Composite Materials
Newark, DE 19711

Dr. J. Duffy
Brown University
Division of Engineering
Providence, RI 02912

Dr. J. L. Swedlow
Carnegie-Mellon University
Department of Mechanical Engineering
Pittsburgh, PA 15213

Dr. V. K. Varadan
Ohio State University Research Foundation
Department of Engineering Mechanics
Columbus, OH 43210

Dr. E. Krokis
University of Pennsylvania
Department of Metallurgy and Materials Science
College of Engineering and Applied Science
Philadelphia, PA 19104

Universities (Con't.)

Dr. Jackson C. S. Yang
University of Maryland
Department of Mechanical Engineering
College Park, MD 20742

Professor T. Y. Chang
University of Akron
Department of Civil Engineering
Akron, OH 44325

Professor Charles W. Bert
University of Oklahoma
School of Aerospace, Mechanical, and Nuclear Engineering
Norman, OK 73019

Professor Satya N. Atluri
Georgia Institute of Technology
School of Engineering and Mechanics
Atlanta, GA 30332

Professor Graham F. Carey
University of Texas at Austin
Department of Aerospace Engineering and Engineering Mechanics
Austin, TX 78712

Dr. S. S. Wang
University of Illinois
Department of Theoretical and Applied Mechanics
Urbana, IL 61801

Industry and Research Institutes

Dr. Norman Hobbs
Kaman AviDyne
Division of Kaman Sciences Corporation
Burlington, MA 01803

Argonne National Laboratory
Library Services Department
9700 South Cass Avenue
Argonne, IL 60440

Industry and Research Institutes (Con't.)

Dr. M. C. Junger
Cambridge Acoustical Associates
54 Rindge Avenue Extension
Cambridge, MA 02140

Dr. V. Gudine
General Dynamics Corporation
Electric Boat Division
Groton, CT 06340

Dr. J. E. Greenspon
J. G. Engineering Research Associates
3831 Hamle Drive
Baltimore, MD 21215

Newport News Shipbuilding and Dry Dock Company
Library
Newport News, VA 23601

Dr. W. P. Bosich
McDonnell Douglas Corporation
5301 Bolsa Avenue
Huntington Beach, CA 92647

Dr. H. H. Abramson
Southwest Research Institute
8500 Culebra Road
San Antonio, TX 78284

Dr. E. C. DeHart
Southwest Research Institute
8500 Culebra Road
San Antonio, TX 78284

Dr. H. L. Baron
Weidlinger Associates
110 East 59th Street
New York, NY 10022

Dr. T. L. Geers
Lockheed Missiles and Space Company
3251 Hanover Street
Palo Alto, CA 94304

Mr. William Caywood
Applied Physics Laboratory
Johns Hopkins Road
Laurel, MD 20810

Industry and Research Institutes (Con't.)

Dr. Robert E. Dunham
Pacific Technology
P.O. Box 148
Del Mar, CA 92014

Dr. M. P. Kamminen
Battelle Columbus Laboratories
505 King Avenue
Columbus, OH 43201

Dr. A. A. Shoukrie
Shoukrie Associates, Inc.
Springlake Research Road
13110 Frederick Road
Woodbine,, MD 21797

Dr. James W. Jones
Swanson Service Corporation
P.O. Box 5413
Huntington Beach, CA 92646

Dr. Robert E. Whitnell
Applied Science and Technology
3344 North Torrey Pines Court
Suite 220
La Jolla, CA 92037

Dr. Kevin Thomas
Westinghouse Electric Corp.
Advanced Reactors Division
P.O. Box 158
Madison, PA 15663

Dr. Bernard Shaffer
Polytechnic Institute of New York
Dept. of Mechanical and Aerospace Engineering
333 Jay Street
Brooklyn,, NY 11021

SECURITY CLASSIFICATION OF THIS PAGE (When Data Entered)

REPORT DOCUMENTATION PAGE		READ INSTRUCTIONS BEFORE COMPLETING FORM
1. REPORT NUMBER UWA/DME/TR-83/47	2. GOVT ACCESSION NO.	3. RECIPIENT'S CATALOG NUMBER
4. TITLE (and Subtitle) Hybrid Experimental-Numerical Stress Analysis		5. TYPE OF REPORT & PERIOD COVERED Technical Report
		6. PERFORMING ORG. REPORT NUMBER UWA/DME/TR-83/47
7. AUTHOR(s) A. S. Kobayashi		8. CONTRACT OR GRANT NUMBER(s) N00014-76-C-0060
9. PERFORMING ORGANIZATION NAME AND ADDRESS Department of Mechanical Engineering FU-10 University of Washington Seattle, WA 98195		10. PROGRAM ELEMENT, PROJECT, TASK AREA & WORK UNIT NUMBERS NR 064-478
11. CONTROLLING OFFICE NAME AND ADDRESS Office of Naval Research Arlington, VA 22217		12. REPORT DATE April 1983 13. NUMBER OF PAGES 30
14. MONITORING AGENCY NAME & ADDRESS(if different from Controlling Office)		15. SECURITY CLASS. (of this report) unclassified 15a. DECLASSIFICATION/DOWNGRADING SCHEDULE

16. DISTRIBUTION STATEMENT (of this Report)

Unlimited

17. DISTRIBUTION STATEMENT (of the abstract entered in Block 20, if different from Report)

18. SUPPLEMENTARY NOTES

19. KEY WORDS (Continue on reverse side if necessary and identify by block number)

Finite element method, Boundary element method, finite difference method, biomechanic, fracture mechanics

20. ABSTRACT (Continue on reverse side if necessary and identify by block number)

The hybrid experimental-numerical stress analysis technique, which saw limited applications during the 1950's, has been resurrected with the vastly improved numerical techniques of the 1970's. By inputing the experimental results as initial and boundary conditions, modern computer codes can be executed in its generation and application modes to yield results which are unobtainable when only one of the two techniques is used. The hybrid technique thus exemplifies the complementary role of the experimental and numerical techniques

DD FORM 1 JAN 73 1473 EDITION OF 1 NOV 65 IS OBSOLETE
S/N 0102-014-6601

Unclassified
SECURITY CLASSIFICATION OF THIS PAGE (When Data Entered)